Effect of Reynolds number on compressible convex-corner flows

Kung-Ming Chung[*1], Po-Hsiung Chang[2a] and Keh-Chin Chang[2b]

[1]*Aerospace Science and Technology Research Center, National Cheng Kung University,
2500 Section 1, Chung-Cheng South Road, Guiren district, Tainan, 711, Taiwan*
[2]*Department of Aeronautics and Astronautics, National Cheng Kung University,
1 University Road, East district, Tainan, 701, Taiwan*

Abstract.   An experimental study was conducted to investigate the effect of Reynolds number on compressible convex-corner flows, which correspond to an upper surface of a deflected flap of an aircraft wing. The flow is naturally developed along a flat plate with two different lengths, resulting in different incoming boundary layer thicknesses or Reynolds numbers. It is found that boundary layer Reynolds number, ranging from 8.04×10^4 to 1.63×10^5, has a minor influence on flow expansion and compression near the corner apex in the transonic flow regime, but not for the subsonic expansion flow. For shock-induced separated flow, higher peak pressure fluctuations are observed at smaller Reynolds number, corresponding to the excursion phenomena and the shorter region of shock-induced boundary layer separation. An explicit correlation of separation length with deflection angle is also presented.

1. Introduction

Aircraft designs have employed flaps for takeoff and landing and ailerons for routine turning maneuver. For a variable camber control wing (Bolonkin and Gilyard 1999), deflected flaps and ailerons can be employed in performance optimization for an aircraft during cruise flight. However, a typical feature on a transonic airfoil is associated with a quasi-normal shock on the upper surface. When the shock is strong enough, development of separation bubble changes the flow field significantly and increases the drag (Delery 1983). A study of Szodruch and Hilbig (1998) indicated that the critical Mach number, onset of boundary layer separation and drag are strongly related to the deflection of control surfaces. Thus there exists a great deal of uncertainty regarding the allowable deflection before separation near the hinge line.

Mason (1993) indicated that there are two fundamental issues regarding the aerodynamic characteristics on upper deflected surfaces, including effect of Reynolds number and transition of

---

∗Corresponding author, Research fellow and Director, E-mail: kmchung@mail.ncku.edu.tw
[a]Ph.D. Student, E-mail: kiby716@gmail.com
[b]Professor, E-mail: kcchang@mail.ncku.edu.tw

expansion flows. For a simplified model of deflected upper control surfaces (convex corners) at high subsonic Mach number M, a typical flow feature is upstream expansion and downstream compression near the corner apex. At higher M and larger convex-corner angle η, the flow switched from subsonic expansion to transonic expansion (Chung 2000, 2002). The downstream boundary layer was separated once the local peak Mach number exceeded 1.3 (Liu and Squire 1987). Unsteadiness of the interaction due to shock excursion phenomenon was characterized by a local peak pressure fluctuation and deviation of higher order moments from effective Gaussian (Chung 2004). The spectrum analysis demonstrated that the unsteady shock motion (or shock excursion) resulted in substantially increased energy level at lower frequencies (Chung 2002). A similarity parameter was also proposed by Chung (2012) to characterize compressible convex-corner flows, including local peak Mach number M_{peak}, peak pressure fluctuations $(\sigma_p/p_w)_{max}$ and shock-induced boundary layer separation length X_i^*.

It is known that blowing is qualitatively equivalent to a decrease in Reynolds number (Inger and Zee 1978). Injection of a small quantity of high-pressure air can energize the incoming boundary layer, thus inducing an increase in displacement thickness or less fuller boundary layer. Chung (2007, 2010) investigated the effect of upstream blowing jet on compressible convex-corner flows. It was found that a small amount of upstream blowing resulted in a delay in transition from subsonic to transonic expansion flows. Lower level of downstream surface pressure fluctuations was also observed in subsonic interactions. In transonic convex-corner flows, larger blowing rates resulted in upstream movement of shock wave and enhanced the flow unsteadiness (or shock-induced boundary layer separation, SIBLS) near the corner. Kim *et al.* (1996) pointed out that SIBLS can be strongly dependent on the way how the variation in Reynolds number was given. The pressure rise up to the separation point decreased as the boundary layer thickness increased at a fixed unit Reynolds number. However, within range of the boundary layer Reynolds number of 10^4 to 10^6, separation pressure rise is insensitive to variation of Reynolds number as the Mach number is relatively small, and essentially independent of Reynolds number for the minimum Mach number necessary to separate the boundary layer.

To investigate quantitatively the effect of Reynolds number on compressible convex-corner flows, a turbulent boundary layer was naturally developed along a flat plate of two different lengths (500 and 275 mm). The boundary layer thickness δ upstream of the corner apex was employed as a characteristic length scale. Surface pressure measurements and surface oil flow visualization were conducted. Before discussing results of the present study, brief details of the experiment are outlined next.

2. Experimental setup

2.1 Transonic wind tunnel and test models

Experiments were conducted in the blowdown transonic wind tunnel at the Aerospace Science and Technology Research Center, National Cheng Kung University (ASTRC/NCKU). This facility includes compressors, a water cooling system, air dryers, storage tanks, and a tunnel. The dew point of the high-pressure air through the dryers is maintained at −40°C under normal operation conditions and air storage volume for the three storage tanks is 180 m^3 at 5.15 MPa. A rotary perforated sleeve valve controls the setup of stagnation pressure p_o, and high-pressure air is discharged into the stilling chamber through flow spreaders. Acoustic baffles, screens and a
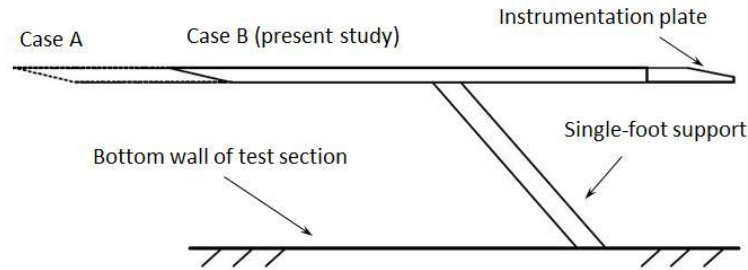
Fig. 1 Test configuration

honeycomb inside the stilling chamber are employed to absorb control-value noise and to reduce flow turbulence intensity. The Mach numbers are varied from 0.2 to 1.4 by exchanging the top and bottom walls of the nozzle. In subsonic test configuration, two choked flaps are employed to control the testing Mach number. Further, the constant-area test section (600 mm×600 mm) enclosed within a plenum chamber was assembled with solid sidewalls and perforated top/bottom walls in this study. M were 0.64, 0.70 and 0.83±0.01, and the unit Reynolds numbers ranged from 20.1 to 23.3 million per meter. The stagnation pressure p_0 and temperature T_0 were 172±0.5 kPa (25 psia) and ambient temperature, respectively.

The test model, which was supported by a single sting mounted on the bottom floor of the test section, comprised a flat plate (150 wide×450 mm long) and an interchangeable instrumentation plate (150 wide×170 mm long), as shown in Fig. 1. The convex corner was 500 mm (Case A) and 275 mm (Case B) from the leading edge of the flat plate. The incoming boundary layer thickness δ at 25 mm ahead of the convex apex was estimated to be approximately 7 mm and 4 mm for Case A and Case B, respectively (Bies 1966). The Reynolds number according to the incoming boundary layer thickness Re_δ ranged from 8.04×10^4 to 1.63×10^5. Five instrumentation plates were fabricated with the convex corner angle η of 5-, 10-, 13-, 15- and 17-deg. One row of 19 pressure taps (6 mm apart) along the centerline of each plate was drilled perpendicularly to the test surface. Further, to prevent cross flow from sidewall interference, two side fences of 13.5 cm (length)×4.5 cm (height)×0.5 cm (thickness) were installed at both sides of the instrumentation plate.

2.2 Instrumentation and data acquisition system

Kulite pressure transducers (XCS-093-25A, B screen) were employed for surface pressure measurements. The sensors had a nominal outer diameter of 2.36 mm and a pressure-sensitive element of 0.97 mm in diameter. External amplifiers (Ecreon Model E713) with a roll-off frequency of approximately 140 kHz were also employed. Test conditions were recorded by a NEFF 620 System while the outputs of pressure transducers were stored by a National Instruments (NI SCXI) system. All input channels were triggered simultaneously with a sampling rate of 200 kHz. Further, the flat-plate cases were employed to estimate experimental uncertainty, which included 1.24% for the normalized surface pressure p_w/p_o and 0.97% for the surface pressure fluctuation coefficient σ_p/p_w.

Surface oil-flow visualization was employed to visualize the surface flow pattern. A thin film of a mixture (titanium dioxide, oil, oleic acid and kerosene) was applied onto the surface of the
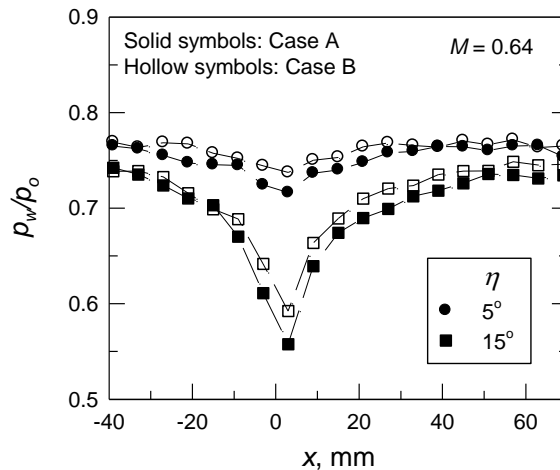
Fig. 2 Wall pressure distributions, subsonic expansion flows

instrumentation plate. For the attached flow, the surface streamlines over the whole span were straight and parallel to the incoming flow direction. With shock-induced, boundary-layer separation, the surface flowfield was not strictly two-dimensional. Accumulation of titanium dioxide was evident followed by the deflection of streamlines. The beginning of accumulation is taken as the separation position and the end of deflection is taken as the reattachment position. The region of separation and reattachment was evaluated and compared with the surface pressure measurements. It is also noted that a motion of the mixture itself on an inclined flat plate owing to gravity effect might contaminate the final flow picture.

3. Results and discussion

3.1 Wall pressure distributions

For compressible convex-corner flows, Ruban *et al.* (2000) demonstrated that the displacement thickness near the corner is affected by the overlapping region that lies between the viscous sublayer and the main part of the boundary layer. For subsonic expansion flows (M=0.64, η=5- and 15-deg), the normalized mean pressure distributions p_w/p_o are shown in Fig. 2, where x denotes the streamwise distance measured along the body surface from the corner apex. It can be seen that there are upstream expansion and downstream compression for both Case A and Case B. The minimum pressure coefficient $(p_w/p_o)_{min}$ is observed immediately downstream of the corner and decreases with increasing η. With decreasing Re_δ (Case B), there is an increase in $(p_w/p_o)_{min}$ (or lower peak mach number) and downstream p_w/p_o. This result agrees with the finding of Chung (2007, 2010) on compressible convex-corner flows with upstream blowing jet. In transonic interactions (M=0.70, η=13-, 15- and 17-deg), the flow accelerates to supersonic and compresses back to subsonic downstream, as shown in Fig. 3. The sonic condition (p_w/p_o=0.5283) is also shown as a dashed line for reference. The distributions of p_w/p_o are almost identical for both test cases and there are slightly lower levels of p_w/p_o near the corner apex for Case B, indicating a
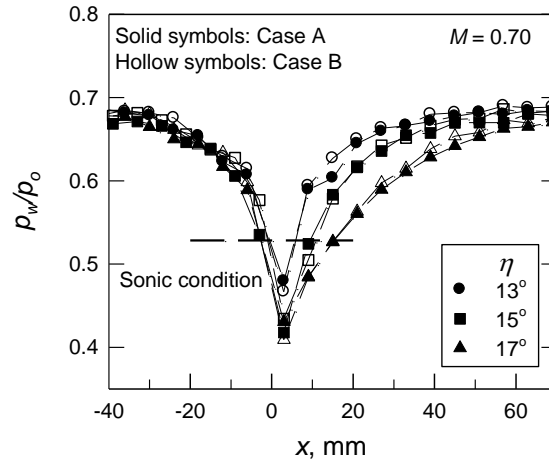
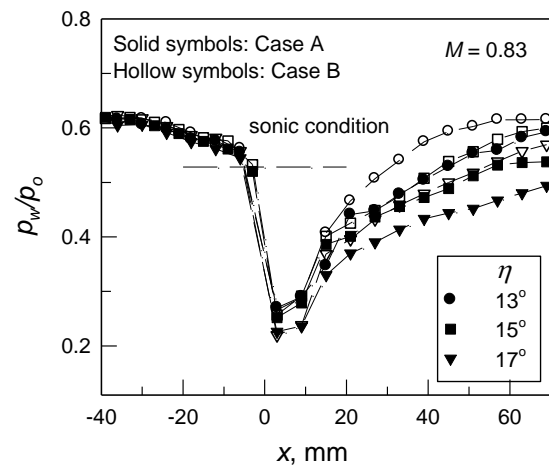Fig. 3 Wall pressure distributions, transonic interactions

Fig. 4 Wall pressure distributions, shock-induced separated flows

minor influence of Re_δ on transonic expansion flows. With increasing freestream Mach number (M=0.83), the test cases at η=13-, 15- and 17-deg correspond to transonic expansion flows with shock-induced, boundary-layer separation, as shown in Fig. 4. The flow either decelerates back to subsonic or remains at supersonic downstream. It is also seen that the Re_δ effect on upstream expansion, $(p_w/p_o)_{min}$ and initial compression is minimized. However, the levels of downstream p_w/p_o increase for Case B.

3.2 Surface pressure fluctuations

To further understand the Re_δ effect on compressible convex-corner flows, the measurements of surface pressure fluctuations are also analyzed. Distributions of surface pressure fluctuations at M=0.64 (η=5-, 10- and 15-deg, subsonic expansion flows) are shown in Fig. 5. For both test cases,
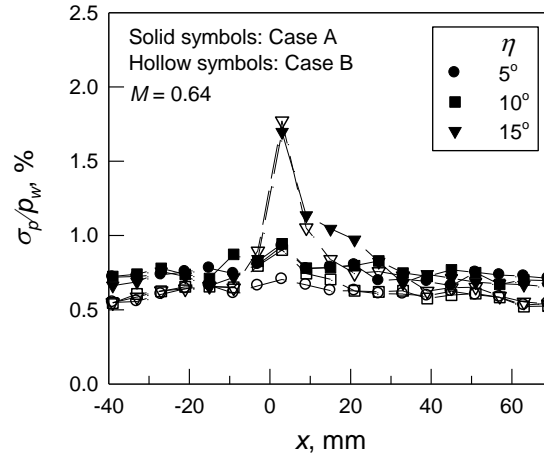
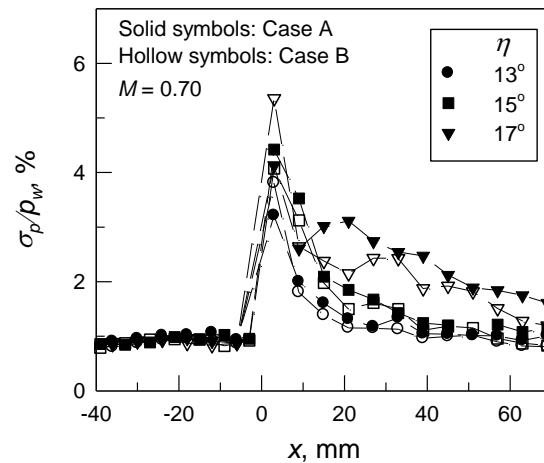Fig. 5 Surface pressure fluctuations, subsonic expansion flows

Fig. 6 Surface pressure fluctuations, transonic interactions

σ_p/p_w increases upstream of the corner and reaches the maxima immediately downstream followed by a decrease to the value of the upstream undisturbed boundary layer. The rise in σ_p/p_w corresponds to flow expansion (or higher local Mach number) near the corner (Laganelli and Martellucci 1983). For Case B, the levels of σ_p/p_w are lower than those of Case A. It is also noted that the Re_δ effect on peak surface pressure fluctuations $(\sigma_p/p_w)_{max}$ is less significant at $\eta = 10$- and 15-deg. In transonic interactions (M=0.70, η=13-, 15- and 17-deg), distributions of σ_p/p_w are shown in Fig. 6. The level of σ_p/p_w upstream of the corner is almost constant for all test cases. With increasing η, the amplitude of $(\sigma_p/p_w)_{max}$ increases for both Case A and Case B. A decrease in Re_δ (Case B) results in an increase in the amplitude of $(\sigma_p/p_w)_{max}$. It is also noted that the amplitude of σ_p/p_w at η=17-deg downstream of the corner is considerably higher than that at lower η and approaches more slowly to some equilibrium level. With SIBLS, $(\sigma_p/p_w)_{max}$ is essentially related to strong adverse pressure gradient and oscillation of the shock wave (Dussauge *et al.* 2006,
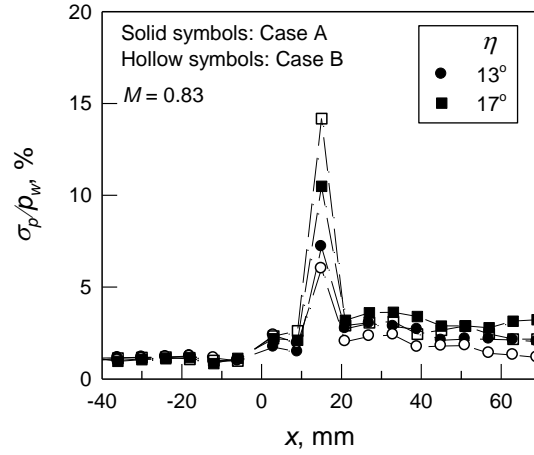
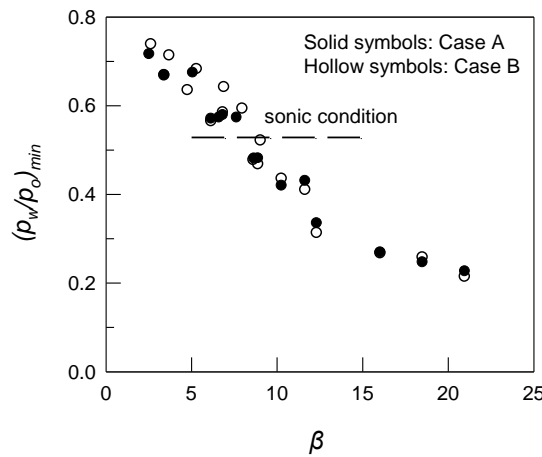Fig. 7 Surface pressure fluctuations, shock-induced separated flows

Fig. 8 Expansion of convex-corner flows

Dussauge and Piponniau 2008, Ogawa *et al.* 2008, Piponniau *et al.* 2009, Wollblad *et al.* 2010, Bernardini *et al.* 2010). Distributions of σ_p/p_w (M=0.83, η=13- and 17-deg) are shown in Fig. 7. It can be seen that surface pressure fluctuations increase upstream of the convex corner and reach the maximum immediately downstream of the corner followed by a sharp decrease. The rapid rise in σ_p/p_w corresponds to boundary layer separation, and higher downstream σ_p/p_w is also a common feature of shock wave/turbulent boundary layer interactions (Dolling 2001). It is also noted that the level of downstream (σ_p/p_w) decreases slightly with decreasing Re_δ.

3.3 Effect of Reynolds number

For compressible convex-corner flows, a similarity parameter $\beta(=M^2\eta/\sqrt{1-M^2}$) was proposed to characterize peak Mach number M_{peak}, SIBLS $X_i{}^*$ and peak pressure fluctuations (Chung 2012).

In Fig. 8, the minimum surface pressure coefficient $(p_w/p_o)_{min}$ is plotted versus β for both Case A and Case B. The amplitude of $(p_w/p_o)_{min}$ appears to be a quadratic function of β. In subsonic expansion flows, higher values of $(p_w/p_o)_{min}$ are observed for Case B, but not for transonic expansion flows with and without SIBLS. Further, the amplitude of M_{peak} is critical on shock structure and flow unsteadiness. A study of Liu and Squire (1987) indicated that flow separation on a circular-arc model at transonic speeds can be classified as trailing-edge separation or shock-induced separation. With a relatively small peak Mach number upstream of the shock wave, boundary layer separation around the trailing edge is owing to adverse pressure gradient. Once reaching the critical peak Mach number (≈ 1.3), the shock wave is strong enough to separate the boundary layer just under the shock foot. Shock excursion results in highly intermittent nature of pressure signals, jumping randomly back and forth. Therefore, for shock-induced separated flows, the undisturbed pressure signals upstream of shock wave were employed to calculate the real M_{peak}. As shown in Fig. 9, the data present a trend similar to that of $(p_w/p_o)_{min}$; that is, the higher M_{peak} the larger β. At $M=0.64$, a decrease in Re_δ results in a decrease in M_{peak}. The flow remains subsonic with β less than 8 and 9 for Case A and Case B, respectively. Reynolds number appears to have a minor effect on flow expansion (or viscous-inviscid interaction) near the corner at $M=0.70$ and 0.83.

In attached flows, a study by Laganelli and Matellucci (1983) indicated that σ_p/p_w is proportional to M^2. With SIBLS, large amplitude of pressure fluctuations is the dominant feature (Dussauge *et al.* 2006). As shown in Fig. 10, the amplitude of $(\sigma_p/p_w)_{max}$ increased with β for the attached and incipient separated flows ($\beta<20$) for both Case A and Case B. The significant increase corresponds to a massive separation of the boundary layer. At lower Re_δ (Case B), low-frequency, unsteady shock motion appears to be triggered at lower β, which agrees with the results previously reported by Chung (2007, 2010). Note that blowing is qualitatively equivalent to a decrease in Reynolds number and larger blowing rates result in upstream movement of shock wave and enhance the flow unsteadiness (or larger peak surface pressure fluctuations) in compressible convex-corner flows.
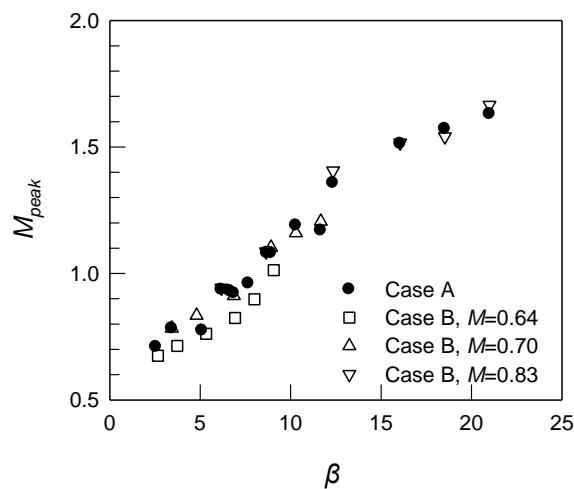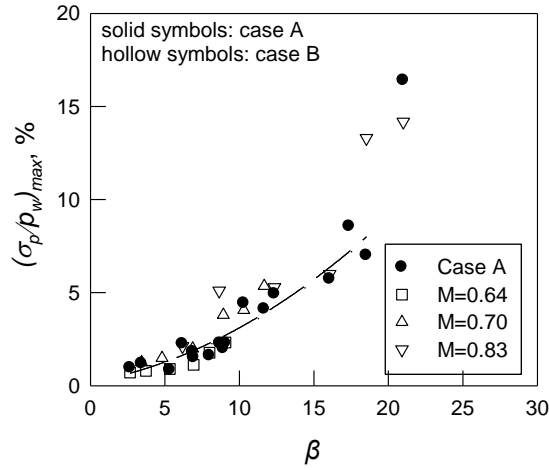

Fig. 9 Peak Mach number
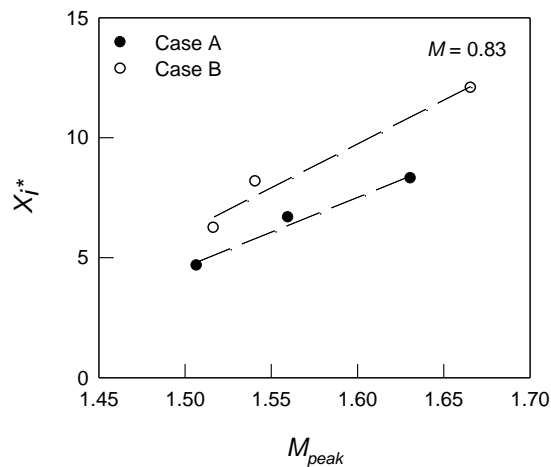
Fig. 10 Peak surface pressure fluctuations

Fig. 11 SIBLS length

SIBLS length X_i is defined as the distance between the separation and reattachment positions, observed by oil flow visualization. At M=0.83, X_i^* increases linearly with M_{peak} (or η) for both Case A and Case B, as shown in Fig. 11. An increase in Re_δ results in a decrease in X_i^*, which is similar to the result by Law (1974) on supersonic ramp flows. It is also noted that Case B has shorter X_i. Chung (2004) proposed that shock excursion could be related to the motion of a separation bubble (expansion and contraction). A decrease in X_i implies higher frequency motion of the separation bubble or higher $(\sigma_p/p_w)_{max}$ as shown in Fig. 10.

For 2- and 3-D compression corner flows, the upstream influence length L_m is usually employed to characterize shock wave/boundary-layer interactions. Settles and Bogdonoff (1983) indicated that the product of upstream influence length and Reynolds number $(L_m/\delta)Re_\delta^{1/3}$ is only a function of ramp angle at a given freestream Mach number. In this study, the product of separation length and Reynolds number $X_i^*Re_\delta^{1/3}$ is re-plotted against β in semi-logarithmic coordinate, as
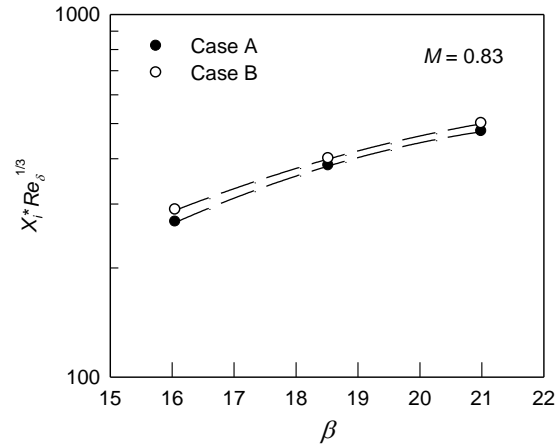
Fig. 12 Re_δ on SIBLS length
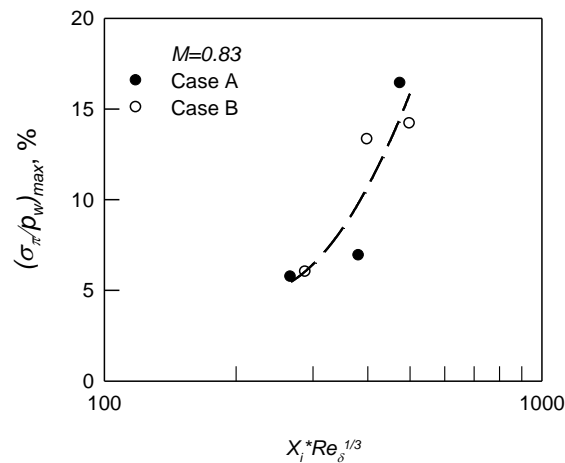
Fig. 13 Re_δ and SIBLS length on peak pressure fluctuations

shown in Fig. 12. As can be seen, $X_i*Re_\delta^{1/3}$ can be correlated with β in a single curve for both Case A and Case B. Further, Chung (2004) indicated that the peak pressure fluctuations of shock-induced separation are associated with the induced separation length. $(\sigma_p/p_w)_{max}$ (M=0.83) is plotted against $X_i*Re_\delta^{1/3}$, as shown in Fig. 13. It appears that $(\sigma_p/p_w)_{max}$ is a second order function of $X_i*Re_\delta^{1/3}$ at a given Mach number.

4. Conclusions

Compressible flow over a convex corner is characterized by upstream expansion and downstream compression. Peak Mach number, peak pressure fluctuations and boundary-layer separation length are associated with freestream Mach number and convex-corner angle. Under the

present test conditions ($Re_\delta = 8.04\times10^4$ to 1.63×10^5), a lower Re_δ resulted in less flow expansion near the corner in subsonic interactions, but not for the test cases of transonic expansion flows with and without SIBLS. There was also a minor variation on the amplitude of upstream surface pressure fluctuations. In transonic expansion flows, peak pressure fluctuations were associated with local peak Mach number and boundary layer separation. A decrease in Reynolds number resulted in a shorter boundary layer separation length, which might enhance the flow unsteadiness or induce larger peak surface pressure fluctuations at a given freestream Mach number and convex-corner angle. The level of downstream surface pressure fluctuations decreased slightly with decreasing Reynolds number. Further, the product of separation length and Reynolds number $X_i*Re_\delta^{1/3}$ at $M=0.83$ can be correlated with β reasonably well.

Acknowledgments

References

Bernardini, A., Pirozzoli, S. and Grasso, F. (2010), "The wall pressure signature of transonic shock/boundary layer interaction", *J. Fluid Mech.*, **671,** 288-312.

Bies, D.A. (1966), "Flight and wind tunnel measurements of boundary layer pressure fluctuations and induced structural response", NASA-CR-626.

Bolonkin, A. and Gilyard, G.B. (1999), "Estimated benefits of variable-geometry wing camber control for transport aircraft", NASA TM-1999-206586, October.

Chung, K.M. (2000), "Transition of subsonic and transonic expansion-corner flows", *J. Aircraft*, **37**(6), 1079-1082.

Chung, K.M. (2002), "Investigation on transonic convex-corner flows", *J. Aircraft*, **39**(6), 1014-1018.

Chung K.M. (2004), "Unsteadiness of transonic convex-corner flows", *Experiment. Fluid.*, **37**(6), 917-922.

Chung, K.M. (2007), "Upstream blowing jet on transonic convex corner flows", *J. Aircraft*, **44**(6), 1948-1953.

Chung, K.M. (2010), "Effect of normal blowing on compressible convex-corner flows", *J. Aircraft*, **47**(4), 1189-1196**.**

Chung, K.M., Chang, P.H. and Chang, K.C. (2012), "Flow similarity in compressible convex corner flows", *AIAA J.*, **50**(4), 985-988.

Delery, J.M. (1983), "Experimental investigation of turbulent properties in transonic shock boundary layer interactions", *AIAA J.*, **21**(11), 1628-1634.

Dolling, D.S. (2001), "Fifty years of shock wave/boundary layer interaction research: what next ?", *AIAA J.*, **39**(8), 1517-1531.

Dussauge, J.P., Dupont, P. and Debieve, J.F. (2006), "Unsteadiness in shock wave boundary layer interactions with separation", *Aero. Sci. Tech.*, **10**(2), 85-91.

Dussauge, J.P. and Piponniau, S. (2008), "Shock/boundary layer interactions: possible sources of unsteadiness", *J. Fluid. Struct.*, **24**, 1166-1175.

Inger, G.R. and Zee, S. (1978), "Transonic shock wave/turbulent boundary layer interaction with suction or blowing", *J. Aircraft*, **15**(11), 750-754.

Kim, H.D., Matsuo, K. and Setoguchi, T. (1996), "Investigation on onset shock-induced separation", *Shock

Waves, **6**(5), 275-286.

Laganelli, A.L. and Martellucci, A. (1983), "Wall pressure fluctuations in attached boundary layer flow", *AIAA J.,* **21**(4), 495-502.

Law, C.H. (1974), "Supersonic, turbulent boundary-layer separation", *AIAA J.*, **12**(6), 794-797.

Liu, X. and Squire, L.C. (1987) "An investigation of shock/boundary layer interactions on curved surfaces at transonic speeds", *J. Fluid Mech.*, **187**, 467-486.

Mason, W.H. (1993), "Fundamental issues in subsonic/transonic expansion corner aerodynamics", *AIAA Paper* 93-0649, January.

Ogawa, H., Babinsky, H., Paetzold, A. and Lutz, T. (2008) "Shock-wave/boundary-layer interaction control using three-dimensional bumps for transonic wings", *AIAA J.*, **46**(6), 1442-1452.

Piponniau, P., Dussauge, J.P., Debieve, J.F. and Dupont, P. (2009), "A simple model for low-frequency unsteadiness in shock-induced separation", *J. Fluid Mech.*, **629**, 87-108.

Ruban, A.I., and Turkyilmaz, I. (2000), "On laminar separation at a corner point in transonic flow", *J. Fluid Mech.*, **423**, 345-380.

Settles, G.S. and Bogdonoff, S.M. (1983), "Scaling of two- and three-dimensional shock/turbulent boundary-layer interactions at compression corners", *AIAA J.*, **20**(6), 782-789.

Szodruch, J., and Hilbig, R. (1988), "Variable wing camber for transport aircraft", *Prog. Aerospace Sci.*, **25**(3), 1988, 297-328.

Wollblad, C., Davidson, L. and Eriksson, L.K. (2010), "Investigation of large scale shock movement in transonic flow", *Int. J. Heat Fluid Flow*, **31**, 528-535.

EC

Nomenclature

M	freestream Mach number
M_{peak}	peak Mach number
p_∞, p_w	mean surface static pressure
q	freestream dynamic pressure
x	coordinate along the surface of the corner, cm
X_i	region of separated boundary layer
X_i*	normalized separation length, X_i/δ
β	similarity parameter, $M^2\eta/\sqrt{1-M^2}$
η	convex-corner angle, deg
δ	incoming boundary layer thickness, mm
σ_p	standard deviation of surface pressure